Simultaneous Hydrogenation of Multiring Aromatic Compounds over NiMo Catalyst

A. R. Beltramone,[†] D. E. Resasco,[†] W. E. Alvarez,[‡] and T. V. Choudhary*,[‡]

CEMS, University of Oklahoma, (OU) 100 East Boyd, Norman, Oklahoma 73019, and Bartlesville Technology Center, ConocoPhillips, Bartlesville, Oklahoma 74004

Hydrogenation of six model feeds containing three-, two-, and one-ring aromatic compounds was investigated to gain insights into the aromatic hydrogenation reaction chemistry over a commercial NiMo catalyst under practical reaction conditions. The hydrogenation reactivity of the aromatic compounds followed the following order: phenanthrene ∼ two-ring aromatics ≫ one-ring aromatic. Comparison with previous studies revealed that the relative reactivity of the aromatic compounds is strongly influenced by the nature of the catalyst. Multiple-component feed studies showed that phenanthrene and naphthalene strongly inhibited the tetralin hydrogenation rate; however, naphthalene and tetralin had no appreciable effect on phenanthrene conversion. Langmuir−Hinshelwood-type rate equations were used to describe the reaction kinetics with physically meaningful and well-identified parameter values. The inhibition was attributed to competitive adsorption and was described in the kinetic model by adsorption terms that were obtained from the multicomponent feed experiments.

Introduction

In recent years, there has been an increasing trend toward processing heavier petroleum crudes.[1] Such crudes typically contain a large number of undesirable aromatic compounds and are considerably more difficult to convert into clean transportation fuels. Meanwhile, due to environmental concern, the worldwide regulations are becoming increasingly stringent.[2−6] Regulations related to aromatic content are especially important in the case of diesel fuels.[7,8] A major process for decreasing the aromatic content of diesel is the hydrogenation of aromatics in a hydrotreating unit. Unfortunately, since petroleum feedstocks with higher aromaticity are being used, it is becoming more challenging to produce low aromatic content diesel fuels. It is therefore highly desirable to increase the efficiency of aromatic hydrogenation. This can be accomplished via process optimization and catalyst improvements, which in turn requires an enhanced understanding about the aromatic hydrogenation process.

The aromatics in diesel feeds can be classified into one-ring, two-ring, and three-ring aromatic compounds. Recent studies from our group have revealed the importance of inhibition between the different aromatic compounds on noble metal catalysts.[9] The investigation demonstrated that the three-ring aromatic compounds considerably inhibited the hydrogenation of the two-ring aromatic and one-ring aromatic compounds over noble metal catalysts. It is important to understand this inhibition effect over hydrotreating catalysts. An interesting study on this topic has been reported by Korre and Klein,[10] wherein they have described the reaction pathways and kinetics for different aromatic compounds and provided some information about the inhibition from different aromatic compounds over a Co-based hydrotreating catalyst. The above referenced study was undertaken in a batch reactor over a $CoMo/Al_2O_3$ catalyst. In practice, commercial diesel hydrotreaters are operated in a continuous flow mode and usually a Ni-based catalyst is preferred for an improved aromatic hydrogenation performance. From a practical viewpoint, it is therefore desirable to obtain insights (extent of inhibition and structure−reactivity−kinetics) into the aromatic hydrogenation process under practical process conditions over a commercial $NiMo/Al_2O_3$ catalyst. With this objective in mind the following has been undertaken in this study: (a) hydrogenation of phenanthrene (three aromatic rings), naphthalene (two aromatic rings), and tetralin (one aromatic ring) as individual component aromatic feeds; (b) hydrogenation of phenanthrene, tetralin, and naphthalene mixtures as multicomponent aromatic feeds; and (c) kinetic modeling of the experimental data.

Efforts have been undertaken to clearly show the inhibition effects from the different aromatic compounds. The experimental study has been undertaken in a continuous flow reactor under industry-relevant temperature (345 °C) and pressure (70 atm)

Table 1. Model Feeds Used in This Study[a]

	feed no. (wt %)					
	1	2	3	4	5	6
tetralin (monoring)	5			5	5	5
naphthalene (diring)		3		3		3
phenanthrene (triring)			2		2	2

[a] Dodecane was used as the solvent.

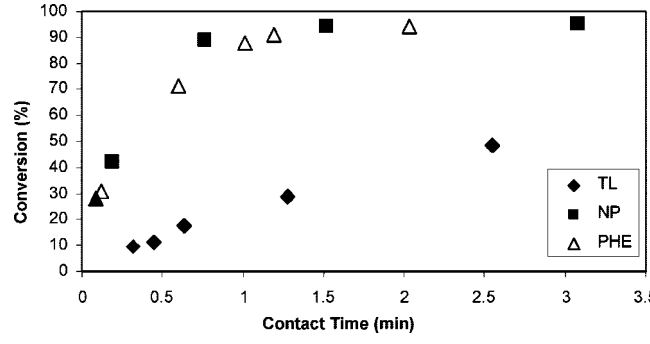

Figure 1. Conversion of tetralin, naphthalene, and phenanthrene over $NiMo/Al_2O_3$ at 1000 psig, 345 °C. Model feeds 1−3 (see Table 1).

* To whom correspondence should be addressed. E-mail: tushar.v.choudhary@conocophillips.com.
[†] University of Oklahoma.
[‡] ConocoPhillips.

10.1021/ie8004258 CCC: $40.75
Published on Web 08/27/2008

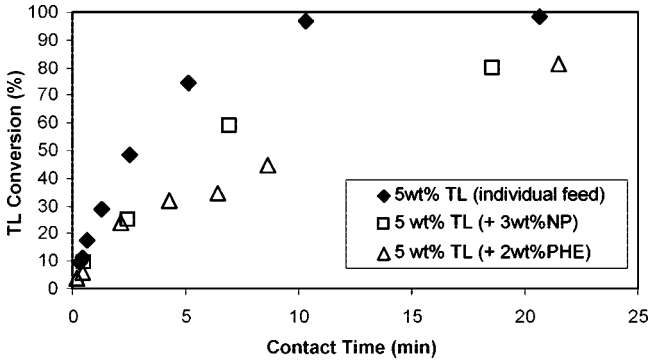

Figure 2. Conversion of tetralin over $NiMo/Al_2O_3$ at 1000 psig, 345 °C. Model feeds 1, 4, and 5 (see Table 1).

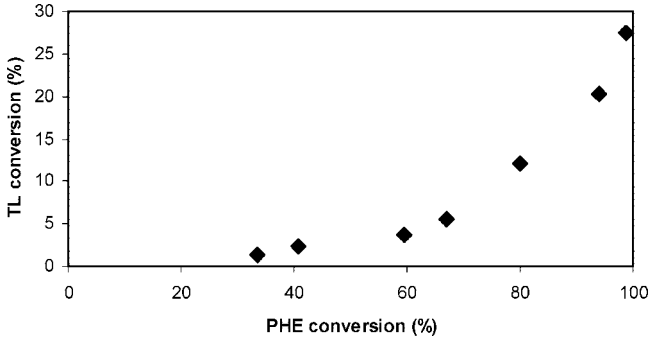

Figure 3. Conversion of tetralin against phenanthrene conversion over $NiMo/Al_2O_3$ at 1000 psig, 345 °C. Model feed 6 (see Table 1).

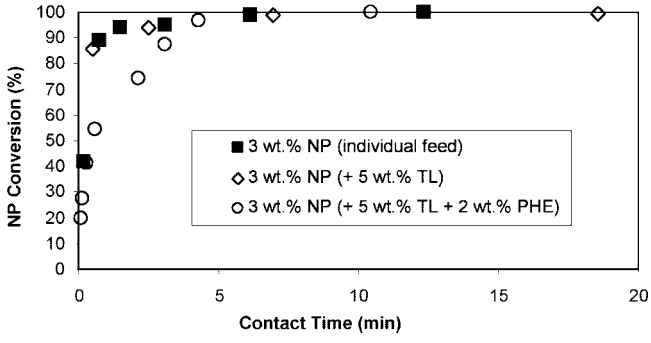

Figure 4. Conversion of naphthalene over $NiMo/Al_2O_3$ at 1000 psig, 345 °C. Model feeds 2, 4, and 6 (see Table 1).

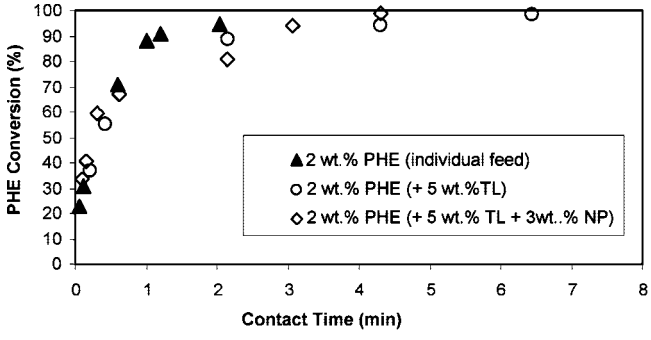

Figure 5. Conversion of phenanthrene over $NiMo/Al_2O_3$ at 1000 psig, 345 °C. Model feeds 3, 5, and 6 (see Table 1).

conditions at different contact times over a commercial $NiMo/Al_2O_3$ catalyst.

Experimental Section

The commercial NiMo/alumina hydrotreating catalyst (Criterion 424) used for the experiments contained 6 wt % Ni and

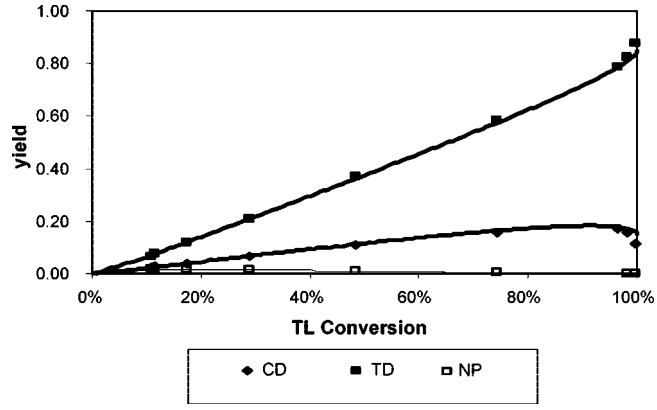

Figure 6. Kinetics of tetralin hydrogenation. Yield vs conversion of TL. Model feed 1 (Table 1). $P = 1000$ psig; $T = 345$ °C. The lines were obtained by fitting the kinetic curves derived from the model to the experimental data.

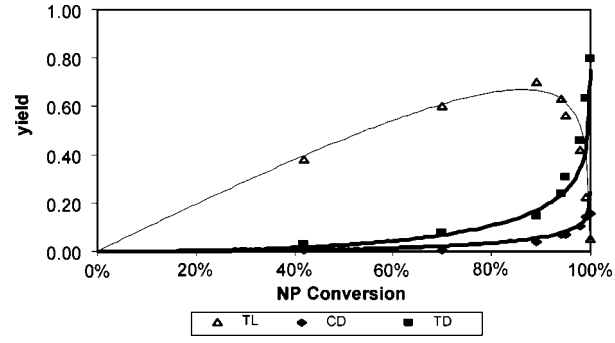

Figure 7. Kinetics of naphthalene hydrogenation. Yield vs conversion of NP. Model feed 2 (Table 1). $P = 1000$ psig; $T = 345$ °C. The lines were obtained by fitting the kinetic curves derived from the model to the experimental data.

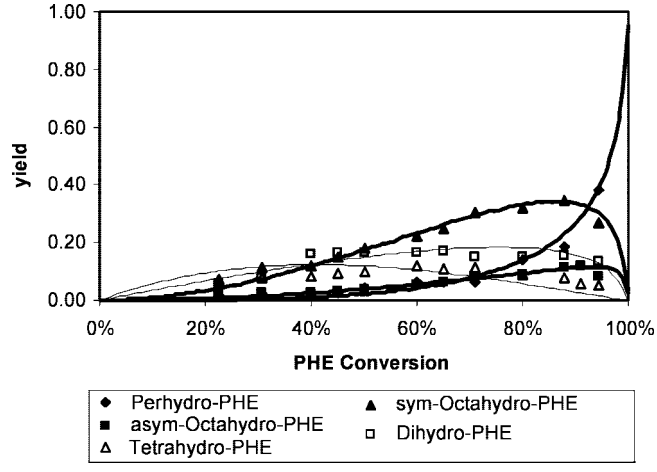

Figure 8. Kinetics of PHE hydrogenation. Yield vs conversion of PHE. Model feed 3 (Table 1). $P = 1000$ psig; $T = 345$ °C. The lines were obtained by fitting the kinetic curves derived from the model to the experimental data.

18 wt % Mo. The catalytic activity was measured in a continuous flow reactor at a temperature of 345 °C and pressure of 70 atm, H_2/HC molar ratio = 20−130, and at different contact times [obtained by dividing mass (weight) of catalyst by mass feed flow], the contact time was varied by changing the amount of catalyst. Experiments were undertaken at predetermined conditions (flow rate 10 mL/h and particle diameter <0.64 mm) where no significant mass-transfer effects were expected. Because of the concentration of the components used (extremely

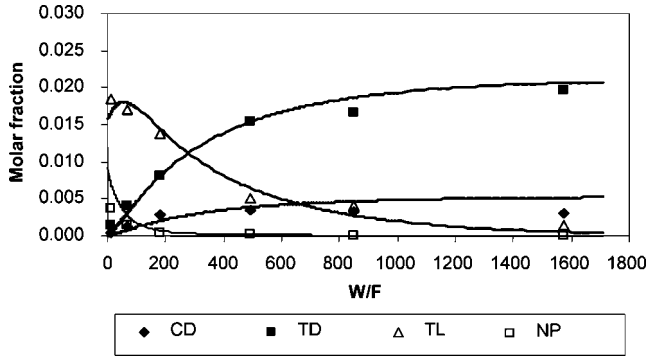

Figure 9. Kinetics of TL+NP hydrogenation. Molar fraction vs W/F (grams of catalyst per hour/mole of TL + NP). Model feed 4. $P = 1000$ psig; $T = 345$ °C. The lines were obtained by fitting the kinetic curves derived from the model to the experimental data.

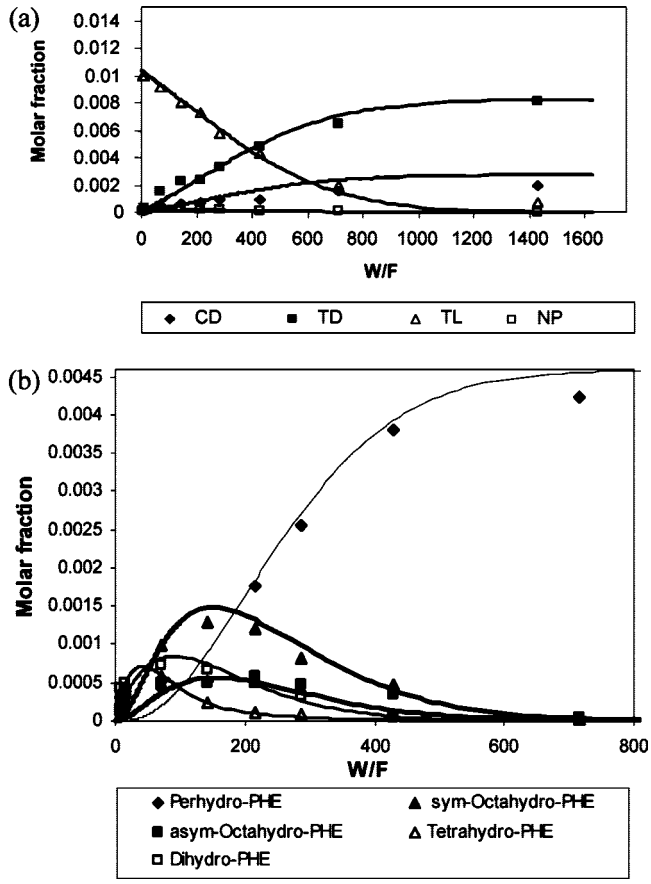

Figure 10. Kinetics of TL + PHE hydrogenation. Molar fraction vs W/F (grams of catalyst per hour/mole of TL+PHE). Model feed 5 (Table 1). $P = 1000$ psig; T=345 °C. (a) TL hydrogenation products; (b) PHE hydrogenation products. The lines were obtained by fitting the kinetic curves derived from the model to the experimental data.

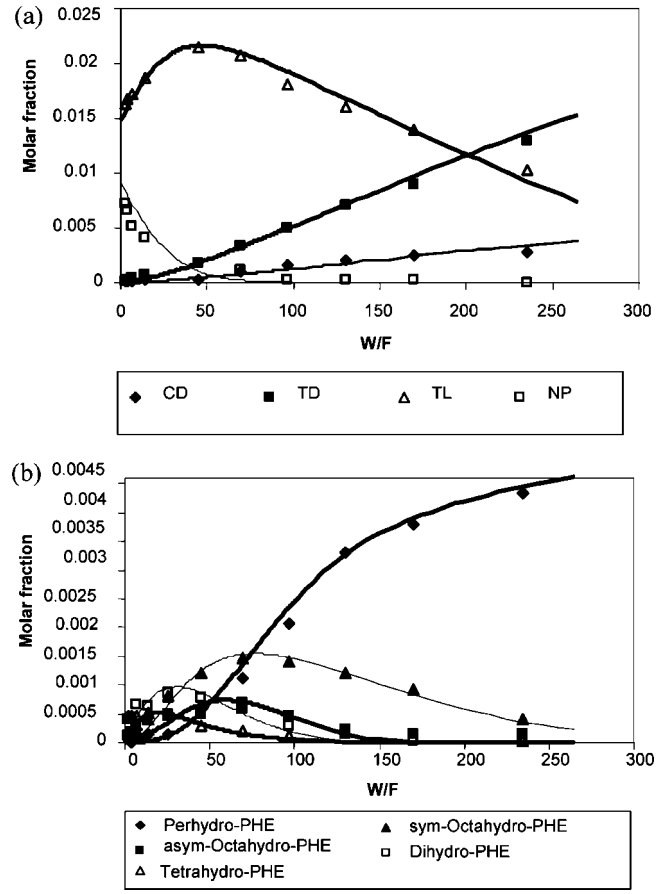

Figure 11. Kinetics of TL + NP + PHE hydrogenation. Molar fraction vs W/F (grams of catalyst per hour/mole of TL + NP + PHE). Model feed 6 (Table 1). $P = 1000$ psig; $T = 345$ °C. (a) TL and NP hydrogenation products; (b) PHE hydrogenation products. The lines were obtained by fitting the kinetic curves derived from the model to the experimental data.

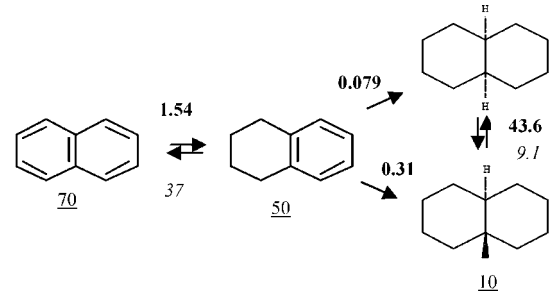

Figure 12. Proposed network for naphthalene/tetralin hydrogenation. Kinetic constant k (mmol/g·cat·h). Adsorption constants K (atm^{-1}) underlined. Equilibrium constants K_{eq} in italics. $n_2 = 2$, $z = 3$, $F = 7.87 \times 10^{-5}$, and estimated deviation 2.60×10^{-5}. $K_{H_2} = 76$ atm^{-1}, obtained from the simultaneous fitting.

rich in H_2), the reaction system is in the gas phase under our operating conditions. Prior to each run, the catalyst sample was physically mixed with 5 mL of inert alumina and placed in the center of the reactor, between layers of 3-mm glass beads. The catalyst was first pretreated in a flow of 10% H_2S in H_2 at 200 and 370 °C. For each sulfiding step, at least five times the stoichiometric number of moles of H_2S required to sulfide the metal components of the catalyst (Ni, 6 wt %; Mo, 18 wt %) was used. Following the sulfiding step, the catalyst was cooled in N_2 flow to ambient temperature. After the pretreatment, 10 mL/h liquid feed was introduced to the reactor using a high-pressure D-500 Isco pump. The effect of time on stream (TOS) on hydrogenation reaction was studied for 24 h over the catalyst at 345 °C with a feed flow of 10 mL/h and 0.5 g of catalyst (20−35 mesh size). The catalytic activity was found to be constant for the first 20 h (no change with time), with subsequent slight deactivation probably due to coke formation. The data were collected at TOS = 5 h, because of the stabiltity and reproducibility of the data at this TOS. The reproducibility of the experimental data was within ±5%. Several different feeds were used in this work (see Table 1). The model feeds were prepared using the following compounds individually or in blends: tetralin (TL; Acros, +98%), naphthalene (NP; Aldrich, +99%), and phenanthrene (PHE; Aldrich, 98%). Dodecane (DO; Aldrich, 99%) was used as the matrix for the model feeds and

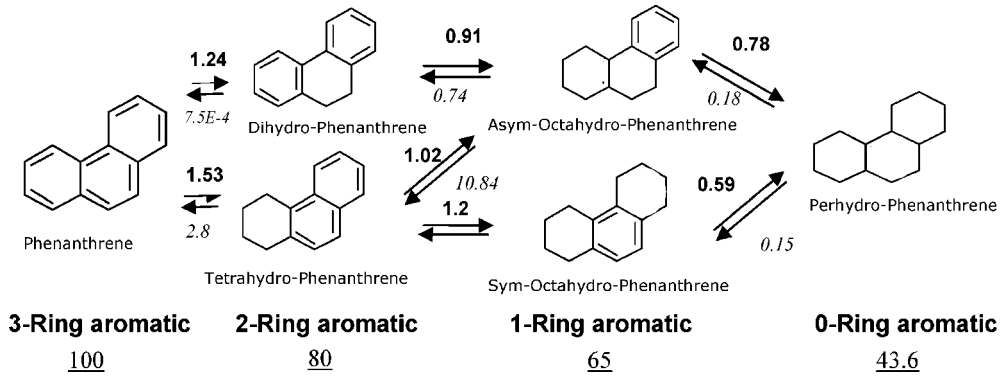

Figure 13. Proposed network for phenanthrene hydrogenation. Kinetic constant k (mmol/g·cat·h). Adsorption constants K (atm^{-1}) underlined. Equilibrium constants K_{eq} in italics. $n_2 = 2$, $z = 3$, $F = 1.27 \times 10^{-5}$, and estimated deviation 7.52×10^{-6}.

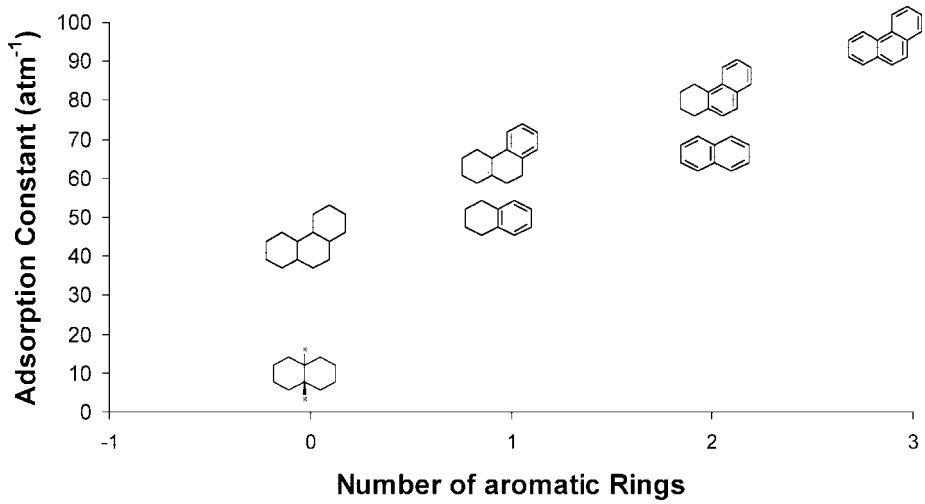

Figure 14. Adsorption constants K (obtained from the kinetic fittings) in function of the number of aromatic rings.

500 ppm of 4,6-dimethyl dibenzothiophene and dibenzothiophene were included as sulfur compounds for each feed. The relative internal distribution of the aromatic compounds (PHE vs NP vs TL content with respect to each other) was chosen such that it represented real diesel feed stocks (low relative content of higher ring aromatic compounds). The total aromatic content was based on experimental limitations (low solubility of PHE in DO, etc). However, we do not believe that a composition change would have affected our conclusions.

The products were trapped with chilled water and analyzed online by a HP6890 gas chromatograph with a FID detector using a HP-5 column and a Shimadzu GCMS-QP5000 with a GC-17A gas chromatograph and AOC-20i autoinjector and HP-5 column 30-m length, 25-mm inner diameter, and 25-μm film thickness.

Results and Discussion

Reactivity of Individual Aromatic Compounds. Figure 1 shows the hydrogenation activity for the individual aromatic compounds (feeds 1−3). The one-ring compounds exhibited significantly lower hydrogenation activity than the two- and three-ring aromatic compounds. While 90+% conversion was obtained for PHE and NP at a contact time of 2.5 min, the conversion of tetralin under identical process conditions was only 45%. At lower contact times (extremely high space velocity), PHE showed lower conversion than NP. However, the conversion for PHE and NP were similar at higher contact times. Based on this study, the reactivity of the aromatic compounds shows the following trend: PHE ∼ NP ≫ TL. In a previous study on Co-based catalyst, PHE was found to have significantly lower reactivity than NP[10] for the hydrogenation of the first aromatic ring, whereas on noble metal catalysts, the PHE was found to have considerably more reactivity than NP.[9] The difference in relative reactivity for the PHE and NP molecules for different catalysts suggests an important interplay between structure of the aromatic molecule and the nature of the active site. Further studies need to be undertaken to understand this intriguing issue.

Inhibition Effects in the Hydrogenation of Aromatics Compounds. Figure 2 shows the tetralin conversion against contact time for the following feeds:

TL in DO (feed 1); TL + NP in DO (feed 4); TL +PHE in DO (feed 5).

The inhibition effect of PHE and NP on TL is clearly observed in this figure. High conversions of TL (>90%) were observed at relatively low contact times for feed 1; however, to obtain similar TL conversions in the mixture feeds (with PHE and NP, feeds 4 and 5), considerably higher contact times were needed. Figure 3 shows the TL conversion as a function of PHE conversion (feed 6). Due to the strong inhibition effect from PHE, the TL conversion was low until extremely high conversions of PHE were reached.

Figure 4 shows the NP conversion against contact time for the following feeds:

NP in DO (feed 2); NP + TL in DO (feed 4); NP + TL + PHE in DO (feed 6).

The NP conversion was similar for the feeds 2 and 4, which indicates that the TL does not inhibit the hydrogenation of NP. However, the presence of PHE in the feed (feed 6) had a distinct detrimental effect on the NP conversion. Figure 5 shows that PHE hydrogenation remains mostly unaffected in feed mixtures containing NP and TL, indicating the absence of any significant inhibiting effect for the PHE hydrogenation reaction. Computational work (described in the next section) was undertaken to shed further light on the inhibition effects described above.

Kinetic Model. The detailed reaction path for TL, NP, and PHE hydrogenation has been described previously.[11] A simplified reaction network for NP, TL, or both takes into account four main reactions: (1) hydrogenation of NP to TL; (2) hydrogenation of TL to *cis*-decalin (CD) (3) hydrogenation of TL to *trans*-decalin (TD), and (4) isomerization of *cis*- and *trans*-decalin. The proposed network for PHE is as follows: (5) hydrogenation of PHE to dihydrophenanthrene and tetrahydrophenanthrene (two aromatic ring); (6) hydrogenation of two-aromatic ring to octahydrophenanthrenes (one aromatic ring); (7) hydrogenation of one-aromatic ring to perhydrophenanthrenes (zero aromatic ring).

Under the conditions of the present study, all the reactions were considered reversible. The semiempirical kinetic model proposed is the generalized Langmuir−Hinshelwood model for hydrogenation suggested by Kiperman.[12] For a generic hydrogenation reaction, the reaction rate is given by

$$r_{ij} = \frac{k_{ij} K_i K_{H2} \left(P_i^{n1} P_{H2}^{n2} - P_j / K_{eq}\right)}{\left(1 + \sum m K_m P_m^{n3}\right)^Z} \tag{1}$$

where r_{ij} (mol g_{cat}^{-1} h^{-1}) is the rate of conversion of compound i to compound j, P (atm) is the partial pressure, k_{ij} (mol g_{cat}^{-1} h^{-1}) is the kinetic rate constant, K_{eq} is the equilibrium constant, and K_m (atm^{-1}) is the adsorption parameter of individual compounds. Usually $n_1 = 1$, Z represents the number of surface sites required for reaction, $n_3 = 0.5$ for atomic adsorption of H_2, and $m = 1$ for molecular adsorption. This model has been frequently used to describe hydrogenation of aromatics. One important assumption behind this model is that the surface reaction is the rate-limiting step. This supposition is true for ~75% of all heterogeneous reactions[13] and has been reported true for hydrogenation of aromatics. The equilibrium constants were obtained using HSC-Chemistry-5.0. Further information about mechanistic studies related to aromatic hydrogenation may be found in refs 14 and 15.

The overall rate of production of a given compound was obtained from the summation of all the conversion rates involving species i. The rate parameters were regressed individually for each compound, with the constraint of nonnegativity. For a given compound, pure component and mixture experimental data were used simultaneously. As a first step, parameter estimation was performed using the product yield versus reactant conversion data involving a particular compound (y_i vs X_i), (Figures 6−8). These relative rates eliminated the Langmuir−Hinshelwood−Hougen−Watson denominators and provided rate parameters that were independent of the mixture composition (eq 2). The numerator rate parameters K_{ij}, including surface reaction and adsorption contributions regressed by eq 2, were then held constant, and eq 1 was used for the estimation of adsorption parameters, K_m, using molar fraction (hydrogen and dodecane are included in the total number of moles) versus time data, simultaneously for all experiments involving a particular compound and for all compounds in the mixture (we only show for the case of the mixtures, Figures 9−11). Approximately 100 data points (all experimental data generated in this study) were used in the analysis. The nonlinear parameter estimation of the kinetic model was performed with the Powell version of the Levenberg−Marquardt algorithm.[16] The differential equation was solved using the EPISODE package of Scientist. The objective function (eq 3) was the sum of the squares of the differences between experimental and calculated mole composition of aromatics compound at the end of the reactor.

$$\frac{dyi}{dXi} = \frac{\sum_j r_{ij}}{\sum_j r_{1j}} = \frac{\sum_j k_{ij}\left(P_i^{n1} P_{H2}^{n2} - P_j / K_{eq}\right)}{\sum_j k_{1j}\left(P_i^{n1} P_{H2}^{n2} - P_j / K_{eq}\right)} \tag{2}$$

$$F = \sum_1^n (y_{exp} - y_{cal})^2 \tag{3}$$

From the figures, it is clear that the model is able to describe the kinetics of the reactions. The values of the reaction parameters and objective function for the simultaneous fitting are presented in Figures 12 and 13.

Hydrogenation of Tetralin and Napthalene. *trans*-decalin, *cis*-decalin, and naphthalene were observed as the products of the tetralin hydrogenation reaction. Figure 6 summarizes the evolution of product distribution for TL as an individual feed, while Figures 9−11 show the data for mixture feeds. TD was obtained with the highest initial selectivity, followed by CD and naphthalene. The trans isomer is a thermodynamically favored product. The trans/cis ratio is important as previous studies[17] have shown that only the cis form of decalin can be ring-opened without cracking on an acid catalyst. Dehydrogenation of tetralin to naphthalene also took place during the hydrogenation of tetralin, even though the experiments were performed far below the thermodynamic equilibrium. The naphthalene formation was dependent on the tetralin concentration and the hydrogenation rate. High tetralin concentration coupled with low hydrogenation rate favored the naphthalene formation. The dehydrogenation was nevertheless a minor reaction, and only traces of naphthalene were formed.

Kinetics parameter estimation for the network of Figure 12 using the tetralin yield versus W/F (grams of catalyst per hour/mole) data and eq 1 is summarized in form of smooth curves in Figure 6. The interconversion between *cis*- and *trans*-decalin was found to be the fastest reaction, but the fact that the trans/cis ratio remains constant indicates that the cis−*tra*ns isomerization does not take place when TL is present in significant concentration. This can be explained in terms of the adsorption constants, since TL has almost a five times larger adsorption constant than the decalins (Figure 12). Jongpatiwut et al.[9] has also reported such a strong site competition in case of aromatic hydrogenation over a PtPd catalyst.

In the product distribution for the hydrogenation reaction of NP, the sequential reaction of NP to TL to decalin is clearly observed (Figure 7). The major hydrogenation products were tetralin, *trans*-decalin, and *cis*-decalin. The experiments showed that tetralin was the primary product or intermediate in the hydrogenation of naphthalene, and no direct conversion of naphthalene to decalns occurred under the conditions studied. The product distribution for the mixed feeds is quite interesting (Figures 9 and 11). Since TL is a product of the hydrogenation of NP, the amount of TL in the products was higher than that in the feed, but immediately after naphthalene was consumed, TL started hydrogenating toward decalins. The inhibition observed in the conversion of TL is mainly due to a competition

with NP (Figure 9 and 11). Based on this, it seems that TL can start being hydrogenated only after essentially all NP has been removed from the feed. In general, the relative reaction rates for the different steps were in good qualitative agreement with the previous studies on the $CoMo/Al_2O_3$ catalyst;[10] however, there was a distinct quantitative difference probably related to the difference in the nature of the active components.

Hydrogenation of Phenanthrene. In Figure 8, the yield of the various hydrophenanthrenes is shown as a function of conversion. At PHE conversions lower than ~30%, the predominant hydrogenation products were the 2-ring aromatics, dihydrophenanthrene and tetrahydrophenanthrene, and 1-ring aromatics, octahydrophenanthrenes. As the PHE conversion increased, the 1-ring aromatics increased, while the concentration of 2 rings passed through a maximum. The saturated 0-ring aromatics increase markedly at higher W/F (Figures 10b and 11b). The observed trend indicates that the hydrogenation of PHE is sequential and involves desorption and readsorption of the partially hydrogenated products. In a previous study over Pt−Pd,[9] the hydrogenation of PHE was also found to be sequential, i.e., three-ring to two-ring to one-ring to naphthenic ring. Similar values were found for the hydrogenation rate of naphthalene and phenanthrene. Interestingly, over a CoMo catalyst (batch reactor), the hydrogenation rate for PHE was actually lower than that of NP.[10] Rate parameters (Figure 13) for hydrogenation of both two- and three-fused aromatic rings were higher than that for the hydrogenation of a single aromatic ring. The effect of saturated rings can be seen from the higher hydrogenation rate of octahydrophenanthrenes compared to tetralin. The terminal ring in tetrahydrophenanthrene was found to hydrogenate faster than the central ring. This may be related to the difficulty in accessing the central ring due to sterical reasons. Similarly, asym-octahydrophenanthrene (aromatic ring in terminal position) was found to hydrogenate more rapidly than sym-octahydrophenanthrene (aromatic ring in central position).

Phenanthrene and two-ring aromatic compounds were found to strongly inhibit the hydrogenation of one-ring aromatic compounds. This may be attributed to competitive adsorption of the different aromatic compounds, such as PHE and NP, that have considerably larger adsorption constants than the monoring compounds such as TL (Figure 14). In line with this, phenanthrene weakly inhibited the two-ring aromatic compounds while phenanthrene itself was not inhibited by the two- and one-ring aromatic compounds. Since the superficial reaction rate constants obtained for NP and PHE hydrogenation were very similar, and much higher than for TL hydrogenation, the observed competitive behavior in the mixtures can be explained in terms of the adsorption constant: $K_{PHE} > K_{NP} > K_{TL}$. The value of the adsorption parameters increased with the number of rings. While this is in qualitative agreement with previous studies,[10] there is a significant quantitative difference (for example, $K_{2R}/K_{1R} = 1.23$ in the present study and $K_{2R}/K_{1R} = 1.04$ in the previous study), which is probably related to the nature of the catalyst employed.

Conclusions

The main findings of the study are summarized below:

a. The reactivity of the model compounds decreased in the order phenantherene ~ napthalene > tetralin, regardless of whether they were hydrogenated separately or as mixtures.

b. Comparison with previous studies revealed that the relative reactivity between phenanthrene and naphthalene was very strongly dependent on the catalyst system employed, indicating that there is a profound relationship between the structure of the aromatic compound and nature of the active site.

c. In mixtures, the hydrogenation rates were significantly affected by the presence of other aromatic compounds. The hydrogenation rates of tetralin were low when naphthalene, phenanthrene, or both were present in the mixture, while the rate of naphthalene hydrogenation was slightly affected by phenanthrene. This was explained in terms of inhibition arising from competitive adsorption.

d. Hydrogenation of multiring aromatic compounds proceeded in a ring-by-ring manner, and the value of the adsorption parameters increased with the number of aromatic rings.

Literature Cited

(1) Gembicki, V. A.; Cowan, T. M.; Brierley, G. R. Update processing operations to handle heavy feedstocks. *Hydrocarbon Process.* **2007**, *86*, 41.

(2) Choudhary, T. V.; Parrott, S.; Johnson, B. Unraveling heavy oil desulfurization chemistry: Targeting clean fuels. *Environ. Sci. Technol.* **2008**, *42*, 1944.

(3) Song, C. S. An overview of new approaches to deep desulfurization for ultra-clean gasoline, diesel fuel, and jet fuel. *Catal. Today* **2003**, *86*, 211.

(4) Choudhary, T. V.; Malandra, J.; Green, J.; Parrott, S.; Johnson, B. Towards clean Fuels: molecular level sulfur reactivity in heavy oils. *Angew. Chem., Int. Ed.* **2006**, *45*, 3299.

(5) Brunet, S.; Mey, D.; Perot, G.; Bouchy, C.; Diehl, F. On the hydrodesulfurization of FCC gasoline: a review. *Appl. Catal., A: Gen.* **2005**, *278*, 143.

(6) Choudhary, T. V. Structure-reactivity-mechanistic considerations in heavy oil desulfurization. *Ind. Eng. Chem. Res.* **2007**, *46*, 8363.

(7) Owusu-Boakye, A.; Dalai, A. K.; Ferdous, D.; Adjaye, J. Maximizing Aromatic Hydrogenation of Bitumen-Derived Light Gas Oil: Statistical Approach and Kinetic Studies. *Energy Fuels* **2005**, *19*, 1763.

(8) Jacquin, M.; Jones, D. J.; Roziere, J.; Lopez, A. J.; R-Castellon, E.; Menado, J. M. T.; Lenarda, M.; Storaro, L.; Vaccari, A.; Albertazzi, S. Cetane improvement of diesel with a novel bimetallic catalyst. *J. Catal.* **2004**, *228*, 447.

(9) Jongpatiwut, S.; Li, Z.; Resasco, D. E.; Alvarez, W. E.; Sughrue, E. L.; Dodwell, G. W. Competitive hydrogenation of poly-aromatic hydrocarbons on sulfur-resistant bimetallic Pt-Pd catalysts. *Appl. Catal., A: Gen.* **2004**, *262*, 241.

(10) Korre, S. C.; Klein, M. T.; Quann, R. J. Polynuclear aromatic hydrocarbons hydrogenation. 1. Experimental reaction pathways and kinetics. *Ind. Eng. Chem. Res.* **1995**, *34*, 101.

(11) Weitkamp, A. W. Stereochemistry and mechanism of hydrogenation of naphthalenes on transition metal catalysts and conformational analysis of the products. *Adv. Catal.* **1968**, *18*, 1.

(12) Kiperman, S. L. Some problems of chemical kinetics in heterogeneous hydrogenation catalysis. *Stud. Surf. Sci. Catal.* **1986**, *27*, 52.

(13) Fogler, H. S. , In *Elements of Chemical Reaction Engineering,* 3rd ed.; Prentice Hall: Upper Saddle River, NJ, 1999.

(14) Stanislaus, A.; Cooper, B. H. Aromatic hydrogenation catalysis: a review. *Catal. Rev. Sci. Eng.* **1994**, *36*, 75.

(15) Rautanen, P. A. Liquid phase hydrogenation of aromatic compounds on nickel catalyst, Teknillinen Korkeakoulu, Helsinki. *Dissertation Abstr. Int., C* **2003**, *64*, 737.

(16) Beltramone, A. R.; Crossley, S.; Resasco, D. E.; Alvarez, W. E.; Choudhary, T. V. Inhibition of HDA and HDS reactions by nitrogen compounds over $NiMo/Al_2O_3$ catalyst. *Catal. Lett.* **2008**, *123*, 181−185.

(17) Santikunaporn, M.; Herrera, J.; Jongpatiwut, S.; Resasco, D. E.; Alvarez, W. E.; Sughrue, E. L. Ring opening of decalin and tetralin on HY and Pt/HY zeolite catalysts. *J. Catal.* **2004**, *228*, 100.

Received for review March 14, 2008
Revised manuscript received May 15, 2008
Accepted July 15, 2008

IE8004258